

# The Genetic Confirmation and Clinical Characterization of *LOXL3*-Associated MYP28: A Common Type of Recessive Extreme High Myopia

Yi Jiang,<sup>1</sup> Lin Zhou,<sup>2</sup> Yingwei Wang,<sup>1</sup> Jiamin Ouyang,<sup>1</sup> Shiqiang Li,<sup>1</sup> Xueshan Xiao,<sup>1</sup> Xiaoyun Jia,<sup>1</sup> Junwen Wang,<sup>1</sup> Zhen Yi,<sup>1</sup> Wenmin Sun,<sup>1</sup> Xiaodong Jiao,<sup>3</sup> Panfeng Wang,<sup>1</sup> J. Fielding Hejtmancik,<sup>3</sup> and Qingjiong Zhang<sup>1</sup>

<sup>1</sup>State Key Laboratory of Ophthalmology, Zhongshan Ophthalmic Center, Sun Yat-sen University, Guangdong Provincial Key Laboratory of Ophthalmology and Visual Science, Guangzhou, China

<sup>2</sup>Department of Ophthalmology, West China Hospital, Sichuan University, Chengdu, China

<sup>3</sup>Ophthalmic Molecular Genetics Section, Ophthalmic Genetics and Visual Function Branch, National Eye Institute, Rockville, Maryland, United States

Correspondence: Qingjiong Zhang, Pediatric and Genetic Eye Clinic, Zhongshan Ophthalmic Center, Sun Yat-sen University, 54 Xianlie Road, Guangzhou 510060, China; [zhangqji@mail.sysu.edu.cn](mailto:zhangqji@mail.sysu.edu.cn) or [zhangqingjiong@gzoc.com](mailto:zhangqingjiong@gzoc.com).

Received: October 21, 2022

Accepted: February 21, 2023

Published: March 14, 2023

Citation: Jiang Y, Zhou L, Wang Y, et al. The genetic confirmation and clinical characterization of *LOXL3*-Associated MYP28: A common type of recessive extreme high myopia. *Invest Ophthalmol Vis Sci.* 2023;64(3):24. <https://doi.org/10.1167/iovs.64.3.24>

**PURPOSE.** In previous studies, biallelic *LOXL3* variants have been shown to cause autosomal recessive Stickler syndrome in one Saudi Arabian family or autosomal recessive early-onset high myopia (eoHM, MYP28) in two Chinese families. The current study aims to elucidate the clinical and genetic features of *LOXL3*-associated MYP28 in seven new families and two previously published families.

**METHODS.** *LOXL3* variants were detected based on the exome sequencing data of 8389 unrelated probands with various ocular conditions. Biallelic variants were identified through multiple online bioinformatic tools, comparative analysis, and co-segregation analysis. The available clinical data were summarized.

**RESULTS.** Biallelic *LOXL3* variants were exclusively identified in nine of 1226 families with eoHM but in none of the 7163 families without eoHM ( $P = 2.97 \times 10^{-8}$ , Fisher's exact test), including seven new and two previously reported families. Seven pathogenic variants were detected, including one nonsense (c.1765C>T/p.Arg589\*), three frameshift (c.39dupG/p.Leu14Alafs\*21; c.544delC/p.Leu182Cysfs\*3, c.594delG/p.Gln199Lysfs\*35), and three missense (c.371G>A/p.Cys124Tyr; c.1051G>A/p.Gly351Arg; c.1669G>A/p.Glu557Lys) variants. Clinical data of nine patients from nine unrelated families revealed myopia at the first visit at about 5 years of age, showing slow progression with age. Visual acuity at the last visit ranged from 0.04 to 0.9 (median age at last visit = 5 years, range 3.5–15 years). High myopic fundus changes, observed in all nine patients, were classified as tessellated fundus (C1) in five patients and diffuse choroidal atrophy (C2) in four patients. Electroretinograms showed mildly reduced cone responses and normal rod responses. Except for high myopia, no other specific features were shared by these patients.

**CONCLUSIONS.** Biallelic *LOXL3* variants exclusively presenting in nine unrelated patients with eoHM provide firm evidence implicating MYP28, with an estimated prevalence of  $7.3 \times 10^{-3}$  in eoHM and of about  $7.3 \times 10^{-5}$  in the general population for *LOXL3*-associated eoHM. So far, MYP28 represents a common type of autosomal recessive extreme eoHM, with a frequency comparable to *LRPAP1*-associated MYP23.

Keywords: MYP28, *LOXL3*, high myopia, variants, genotype-phenotype

High myopia (HM), a common cause of vision impairment and acquired blindness, is defined as having a spherical equivalent refractive error of  $-6.00$  diopter (D) or greater, as well as an axial length of more than 26 mm.<sup>1</sup> The etiology of HM remains unclear because multiple factors are involved in myopia development including environmental and genetic factors.<sup>2,3</sup> However, early-onset high myopia (eoHM), which is characterized by preschool onset and familial clustering, is considered to be predominantly affected by genetic factors.<sup>4,5</sup> To date, variants in at least 16

genes have been reported to contribute to nonsyndromic Mendelian high myopia whereas variants in at least 84 genes might contribute to syndromic high myopia.<sup>4</sup> Variants in these genes only contributed to a small proportion of families with eoHM based on our previous studies, about 5.6% eoHM is due to genes<sup>6</sup> responsible for nonsyndromic eoHM and about 23% of eoHM is due to genes responsible for syndromic eoHM.<sup>7</sup> Of these, variants in *ARR3* are the most common cause of nonsyndromic eoHM.

Of these genes, *LOXL3* is of special interest because it is one of only two genes identified so far responsible for autosomal recessive eoHM (the other one being *LRPAP1*).<sup>8</sup> *LOXL3*, mapping to chromosome 2p13.3, encodes a protein functioning as a copper-dependent amine oxidase.<sup>9</sup> Biallelic missense variants in *LOXL3* were initially identified in one family with autosomal recessive Stickler syndrome from Saudi Arabia,<sup>10</sup> in which the two patients had eoHM and systemic signs. Subsequently, biallelic truncation variants in *LOXL3* were detected in two Chinese families with autosomal recessive eoHM alone in our previous study,<sup>11</sup> which was designed as MYP28 (OMIM 619781). MYP28 with biallelic *LOXL3* truncation variants was further supported by an additional study with one Saudi Arabian family.<sup>12</sup> Stickler syndrome caused by biallelic missense variants was further supported by an additional family from United Arab Emirates in which one patient had high myopia whereas the other only had low myopia in one eye and low hyperopia in the other eye.<sup>13</sup> It would be interesting to know whether the phenotypic variability is due to the difference in variants (missense vs. truncations) or observational bias.

In the current study, biallelic *LOXL3* variants were identified in nine unrelated families with eoHM (seven new and two previously reported families), but in none of 7163 families without eoHM ( $P = 2.97 \times 10^{-8}$ ), providing firm evidence to support the causative association of MYP28 with *LOXL3* truncation variants. Careful reevaluation of the clinical data from the nine patients from nine unrelated families demonstrated that extreme eoHM is the only prominent and consistent feature in these patients, although typical signs for Stickler syndrome were not observed in these patients at the age of examination. Based on the time of examination results, the initial diagnosis of eoHM is considered preferable for these nine patients with biallelic *LOXL3* variants. Our data suggest that *LOXL3*-associated MYP28 is a common form of autosomal recessive eoHM, with a frequency comparable to *LRPAP1*.<sup>8</sup>

## METHODS

### Subjects and Clinical Data Collection

All probands with a variety of eye disorders and their family members were recruited in the Pediatric and Genetic Eye Clinic, Zhongshan Ophthalmic Center, Guangzhou. Before the collection of clinical data and peripheral venous blood samples of participants, an informed consent document has been obtained from all participants or their guardians, which was voluntarily signed in accordance with the tenets of the Declaration of Helsinki. Our study was approved by the institutional review board of Zhongshan Ophthalmic Center. Genomic DNA was extracted from leukocytes acquired from the peripheral venous blood as described in the previous study.<sup>14</sup>

A routine ophthalmic examination has been conducted on each participant. Further specific ocular and systemic examinations were performed on patients when necessary, including optic coherence tomography (OCT), fundus photography, scanning laser ophthalmoscopy, fundus autofluorescence (FAF), electroretinography (ERG), and radiography. The foveal hypoplasia grade was according to the Leicester Grading System for foveal hypoplasia.<sup>15</sup> Additionally, the myopic fundus classification was based on a simplified classification and grading system for myopic maculopathy proposed by Ohno-Matsui et al.<sup>16</sup>

### Variant Detection and Assessment

Whole-exome sequencing<sup>17</sup> or targeted-exome sequencing<sup>18</sup> was conducted on the genomic DNA of 8389 probands including 1226 with early-onset high myopia and 7163 with other eye conditions (Supplementary Fig. S1). For whole-exome sequencing, exome capture was performed with an Agilent SureSelect Human All Exon Enrichment Kit V4 (Agilent, Santa Clara, CA, USA) array. An Agilent Technologies 2100 Bioanalyzer was used to evaluate the quality of the library and an Illumina HiSeq 2000 system (Illumina, San Diego, CA, USA) was used for library sequencing with an average depth of at least 125-fold. The sequence reads were mapped to the UCSC hg19 genome using the Burrows-Wheeler Aligner software (<http://bio-bwa.sourceforge.net/>). Then variants were called using GATK (<https://gatk.broadinstitute.org/hc/en-us>) and SAMTOOLS (<http://samtools.sourceforge.net/>) implementing Bayesian approaches and annotated using ANNOVA (<http://annovar.openbioinformatics.org/en/latest/>).

For targeted-exome sequencing, the genomic DNA was fragmented using a Bioruptor Plus (Diagenode, Liege, Belgium) to a fragment size of approximately 200 base-pair (bp). The fragments were then processed through a KAPA HTP Library Preparation Kit (Roche, Basel, Switzerland) to generate a paired-end library. Library capture was performed with a NimbleGen SeqCap EZ Choice Library SR V5 kit (Roche), and library sequencing was subsequently completed with an Illumina NextSeq550 Mild output v2 kit (150 bp paired-end) on an Illumina NextSeq550 Analyzer (Illumina, San Diego, CA, USA). Variant calling and annotation data analysis were performed using the StrandNGS software (Karnataka, India). The gene list of the target gene panel is shown in Supplementary Table S1, which has been described in our previous study.<sup>19</sup>

The detected variants in *LOXL3* were screened by multi-steps of bioinformatics analysis. First, low sequencing quality variants with coverage of less than five were excluded. Subsequently, synonymous variants and variants in non-coding regions without impact on splicing signals, which were precomputed by human splicing finder program (<https://hsf.genomnis.com/mutation/analysis/>), were excluded. Variants with high minor allele frequency of 0.01 or more in the gnomAD database (<https://gnomad.broadinstitute.org/>) were also excluded. Then the remaining variants underwent evaluation from five in silico tools: SIFT (<http://sift.jcvi.org/>), Polyphen-2 (<http://genetics.bwh.harvard.edu/pph2/>), PROVEAN ([http://provean.jcvi.org/seq\\_submit.php](http://provean.jcvi.org/seq_submit.php)), CADD (<http://cadd.gs.washington.edu>), and REVEL (<https://sites.google.com/site/revelgenomics/>). Last, variants were classified as likely pathogenic variants after the comparison analysis with the gnomAD database and Human Gene Mutation Database (HGMD). The candidate biallelic variants were validated by the Sanger sequencing following the method described in the previous study.<sup>20</sup> The primers of candidate variants in *LOXL3* (NM\_032603.5 for mRNA) were designed by primer 3 (<http://primer3.ut.ee/>), and further co-segregation analysis was performed on the available family members.

### Haplotype Analysis

Four different 5'-fluorescently labeled microsatellite markers located on chromosome 2p, including D2S2368, D2S286, D2S2333, and D2S2216, were used for analyzing allelic

association in samples from patients with the recurrent *LOXL3* variant. These microsatellite markers were from the ABI Prism Linkage Mapping Set Version 2 (PE Applied Biosystems, Foster City, CA, USA). The PCR process has been described in the previous study.<sup>21</sup> The amplified products were subsequently detected via capillary electrophoresis on the ABI 3500 Genetic Analyzer (Applied Biosystems), The genotyping analysis was performed using GeneMapper ID-X V 1.4 software.

### Statistical Analysis

All statistical analyses in this study were performed using *IBM SPSS Statistics V26.0 software* (Armonk, NY: IBM Corp). The  $\chi^2$  test or Fisher's exact test was applied to compare the frequency of biallelic *LOXL3* variants among 1226 individuals with eoHM and 7163 individuals with other eye conditions in our cohort. The statistical significance was defined as  $P < 0.05$ .

According to our recent study,<sup>6</sup> candidate pathogenic variants in three genes (*LRPAP1*, *OPN1LW*, *ARR3*) have been suggested as causative variants for Mendelian eoHM. Additionally, *LOXL3* variants also have been reported to contribute to eoHM. The keywords "*LOXL3*", "*LRPAP1*", "*OPN1LW*", "*ARR3*," and "high myopia" were searched on PubMed and Google Scholar, and references in English related to this topic were collected. Furthermore, publications linked to variants in these four genes in the HGMD database were reviewed before September 1, 2022, and collected articles related to variants responsible for eoHM. Correspondingly, we summarized the eoHM family numbers of variants in these four genes, the variant frequency, and genotype-phenotype correlations.

## RESULTS

### Molecular Analysis

After multiple bioinformatics analyses performed on the in-house exome sequencing data, biallelic *LOXL3* variants were exclusively clustered in nine unrelated families with eoHM including seven new and two previously reported families, accounting for nine of 1226 probands with eoHM in the cohort, but in none of 7163 families with other eye conditions ( $P = 2.97 \times 10^{-8}$ , Fisher's exact test) (Table 1; Table 2; Supplementary Table S2a). In total, we identified seven variants in the nine families, including three missense variants (c.371G>A/p.Cys124Tyr; c.1051G>A/p.Gly351Arg; c.1669G>A/p.Glu557Lys) and four truncation variants (c.39dupG/p.Leu14Alafs\*21; c.544delC/p.Leu182Cysfs\*3; c.594delG/p.Gln199Lysfs\*35; 1765C>T/p.Arg589\*) (Table 1). All seven variants in our cohort were confirmed by Sanger sequencing (Fig. 1A). The three missense variants were predicted to be pathogenic by at least five in silico tools (Table 1). Of the seven variants, three were absent in the gnomAD database whereas four were extremely rare with allele frequency below 0.0001 (Table 1). None of the variants were found in a homozygous state in the gnomAD database. Based on the above evidence, these seven variants were classified as pathogenic or likely pathogenic variants. Interestingly, the same truncation variant (c.39dupG/p.Leu14Alafs\*21) was identified in eight of nine probands. Haplotypes were constructed by genotyping data of four microsatellite markers and the c.39dupG variant (Supplementary Fig. S2). Haplotype

TABLE 1. Rare Variants in *LOXL3* Predicted To Be Potential Damaging

| Position at Chr2 (GRCh37) | Exon | NM_032603.3 Change | NM_032603.3 Effect | REVEL Score | CADD Score | SIFT Score | Polyphen-2 Score | PROVEAN Pred | GnomAD Allele | Family ID  |
|---------------------------|------|--------------------|--------------------|-------------|------------|------------|------------------|--------------|---------------|--|
| 1                         | 2    | 74779723 c.39dupG  | p.(Leu14Alafs*21)  | /           | /          | /          | /                | /            | 12/253784     | F1;F2;F3;F5;F6;F7; HM293 <sup>†</sup> ; HM407 <sup>†</sup> |
| 2                         | 3    | 74777418 c.371G>A  | p.(Cys124Tyr)      | 0.959       | 27.9       | D (0.000)  | PD (0.996)       | D (-9.540)   | /             | F4   |
| 3                         | 4    | 74776644 c.544delC | p.(Leu182Cysfs*3)  | /           | /          | /          | /                | /            | /             | F1   |
| 4                         | 4    | 74776594 c.594delG | p.(Gln199Lysfs*35) | /           | /          | /          | /                | /            | /             | HM407 <sup>†</sup>   |
| 5                         | 6    | 74763460 c.1051G>A | p.(Gly351Arg)      | 0.586       | 27.9       | D (0.001)  | PD (1.000)       | D (-6.790)   | 9/251152      | F2   |
| 6                         | 10   | 74761812 c.1669G>A | p.(Glu557Lys)      | 0.523       | 30.0       | D (0.000)  | PD (0.986)       | D (-3.740)   | 1/251390      | F3   |
| 7                         | 10   | 74761716 c.1765C>T | p.(Arg589*)        | /           | /          | /          | /                | /            | 2/251256      | F4   |

PD, probably damaging; PB, possibly damaging; D, damaging; B, benign; T, tolerant; N, neutral; DM, damaging mutation; /, not available; For *LOXL3* in gnomAD, 5% variants had REVEL or CADD scores greater than 0.541 or 29.375, while 75% had such scores less than 0.238 or 25.5.

<sup>†</sup>The families HM409 and HM293 were reported in our previous report, whereas the families F1-7 have not been reported previously. The biallelic *LOXL3* variants were detected in five probands from five families (F1; F4; F5; F6; F7) by Target-exome sequencing and in four probands from four families (F2; F3; HM293; HM407) by whole-exome sequencing.



TABLE 2. Clinical Information of the Probands and Affected Siblings With Biallelic LOXL3 Variants Identified in This Study (NM\_032603.5)

| Family ID  | Nucleotide Acid Change | Amino Acid Effect                    | Gender | Age (y) at Exam | Initial Symptom | SER    |        |      | BCVA             |              |    | ERG |             |             | Fundus      |             |    |
|------------|------------------------|--------------------------------------|--------|-----------------|-----------------|--------|--------|------|------------------|--------------|----|-----|-------------|-------------|-------------|-------------|----|
|            |                        |                                      |        |                 |                 | OD     | OS     | OD   | OS               | OD           | OS | OD  | OS          | OD          | OS          | OD          | OS |
| F1-II:1    | c.[39dupG]; [544delC]  | p.[Leu14Alafs*21]; [Leu182Cysfs*3]   | M      | 3               | PV              | -11.75 | -11.50 | 0.12 | 0.10             | NA           | N  | MR  | TF          | TF          | TF          | TF          |    |
| F2-II:2    | c.[39dupG]; [1051G>A]  | p.[Leu14Alafs*21]; [Gly351Arg]       | M      | 4               | PV              | -10.75 | -11.25 | 0.3  | 0.3              | FVH Grade I  | N  | MR  | TF; FVH     | TF; FVH     | TF; FVH     | TF; FVH     |    |
| F3-II:1    | c.[39dupG]; [1669G>A]  | p.[Leu14Alafs*21]; [Glu557Lys]       | F      | 3               | PV              | -13.00 | -13.00 | NA   | NA               | NA           | NA | NA  | DCA         | DCA         | DCA         | DCA         |    |
| F4-II:1    | c.[37IG>A]; [1765C>T]  | p.[Cys124Tyr]; [Arg589*]             | M      | 14              | RD <sup>†</sup> | -20.00 | -20.00 | 0.5  | 0.01             | NA           | NA | NA  | NA          | DCA; PC     | DCA; PC     | DCA; PC     |    |
| F5-II:1    | c.[39dupG]; [39dupG]   | p.[Leu14Alafs*21]; [Leu14Alafs*21]   | M      | 8               | PV              | -15.50 | -15.50 | 0.9  | 0.7              | FVH Grade II | NA | NA  | TF; PC; FVH | TF; PC; FVH | TF; PC; FVH | TF; PC; FVH |    |
| F6-II:2    | c.[39dupG]; [39dupG]   | p.[Leu14Alafs*21]; [Leu14Alafs*21]   | F      | 1.5             | PV              | -12.25 | -13.50 | 0.7  | 0.8 <sup>‡</sup> | NA           | NA | NA  | TF          | TF          | TF          | TF          |    |
| F7-II:2    | c.[39dupG]; [39dupG]   | p.[Leu14Alafs*21]; [Leu14Alafs*21]   | M      | 4               | PV              | -11.75 | -13.50 | 0.3  | 0.3              | FVH Grade I  | N  | MR  | TF          | TF          | TF          | TF          |    |
| HM293-II:1 | c.[39dupG]; [39dupG]   | p.[Leu14Alafs*21]; [Leu14Alafs*21]   | M      | 3               | PV              | -19.25 | -19.00 | NA   | NA               | NA           | NA | NA  | DCA         | DCA         | DCA         | DCA         |    |
| HM407-II:1 | c.[39dupG]; [594delG]  | p.[Leu14Alafs*21]; [Gln1991Lysfs*35] | M      | 15              | RD <sup>‡</sup> | NA     | -24.75 | HM   | 0.04             | NA           | NA | NA  | NA          | NA          | NA          | DCA; PC     |    |

SER, spherical equivalent refractive errors; M, male; F, female; N, normal; NA, not available; PV, poor vision; RD, retinal detachment; HM, hand movement; FVH, foveal hypoplasia; TF, tessellated fundus; PC, peripapillary crescent; DCA, diffuse chorioretinal atrophy; MR, mildly reduced.

Above data are based on available clinical data from patients with LOXL3 variants.

<sup>†</sup> The visual acuity examination was performed on the proband F6-II:1 at the age of five years.

<sup>‡</sup> The left eye of the proband F4-II:1 was hit by a soccer ball and then was found to have rhegmatogenous retinal detachment in the left eye; the right eye of the reported proband HM407-II:1 was observed to have retinal detachment caused by ocular trauma.

analysis in the eight families implied that a potential founder effect might be considered between families F7 and HM293, as well as between F2 and HM407 (Supplementary Fig. S2). Conversely, the c.39dupG variant in the remaining four families was likely derived from different origin or as a recurrent event because they showed completely different haplotypes (Supplementary Fig. S2). Of the nine patients with biallelic *LOXL3* variants, all had at least one truncation allele, including six with biallelic truncations (including four homozygous) and three with one truncation and one missense allele (Fig. 1A; Table 2; Supplementary Fig. S2).

Based on data from our cohort, the estimated prevalence of *LOXL3*-associated eoHM is about  $7.3 \times 10^{-3}$  (9/1226) in eoHM population and is approximately  $7.3 \times 10^{-5}$  in the general population if the prevalence of eoHM is estimated to be 1% in the general population (Supplementary Table S2b). To date, three loci for autosomal recessive eoHM have been mapped, of which variants in *LRPAP1* and *LOXL3* have been identified in MYP23 and MYP28 but not in MYP18. Taking into consideration of pathogenic and likely pathogenic variants with curation based on the large dataset in our cohort and with reference to previously published data for *ARR3*, *OPN1LW*, *LOXL3*, and *LRPAP1*,<sup>6,8,10-13,22-31</sup> variants in *LOXL3* appear to be the third most common cause of eoHM and potentially a common cause of autosomal recessive eoHM (Fig. 1, Supplementary Tables S3, S4).

## The Clinical Phenotypic Features

The clinical characteristics of nine patients with variants in *LOXL3* are briefly presented in Table 2. The main initial symptom was nearsightedness without photophobia except for the proband F4-II:1 and the proband HM407-II:1. The main complaint of F4-II:1 was rhegmatogenous retinal detachment in the left eye due to a soccer ball hit, but the medical record showed that his spherical equivalent refraction was -20.00 diopters in both eyes before retinal detachment. Similarly, the chief complaint of HM407-II:1 was retinal detachment in the right eye due to ocular trauma, but the patient had developed high myopia in both eyes before the age of seven as previously reported.<sup>11</sup> Among these patients, the best corrected visual acuity (BCVA) at the last visit ranged from 0.04 to 0.9 (median = 0.5, decimal), and the median age at the last visit was five years (range 3.5–15 years) (Fig. 2B). Based on available optometry reports of these probands at the first visit (17 eyes of nine individuals), the average spherical equivalent was  $-14.99 \pm 4.06$  diopters (range -10.75 to -24.75 diopters), and the median age at the first visit was five years (Supplementary Table S5; Fig. 2A). According to a follow-up study of retinoscopy results, the MYP28 associated with *LOXL3* showed nonprogressive myopia, characterized by a slow progression of refraction error and steady improvement of BCVA (Fig. 2).

According to the available clinical data, the fundus photography examination revealed classical myopic fundus in 17 eyes of these nine patients (Fig. 3). Based on the myopic maculopathy classification,<sup>16</sup> tessellated fundus (Category 1) was observed in 10 eyes from five patients, and diffuse choroidal atrophy (Category 2) was observed in seven eyes from four patients. Furthermore, the myopic peripapillary crescent was detected in five eyes from three patients, posterior staphyloma was detected in one eye from one patient, and none were found to have choroidal neovascularization, radial perivascular chorioretinal degeneration, radial or circumferential lattice degeneration (Fig. 3;

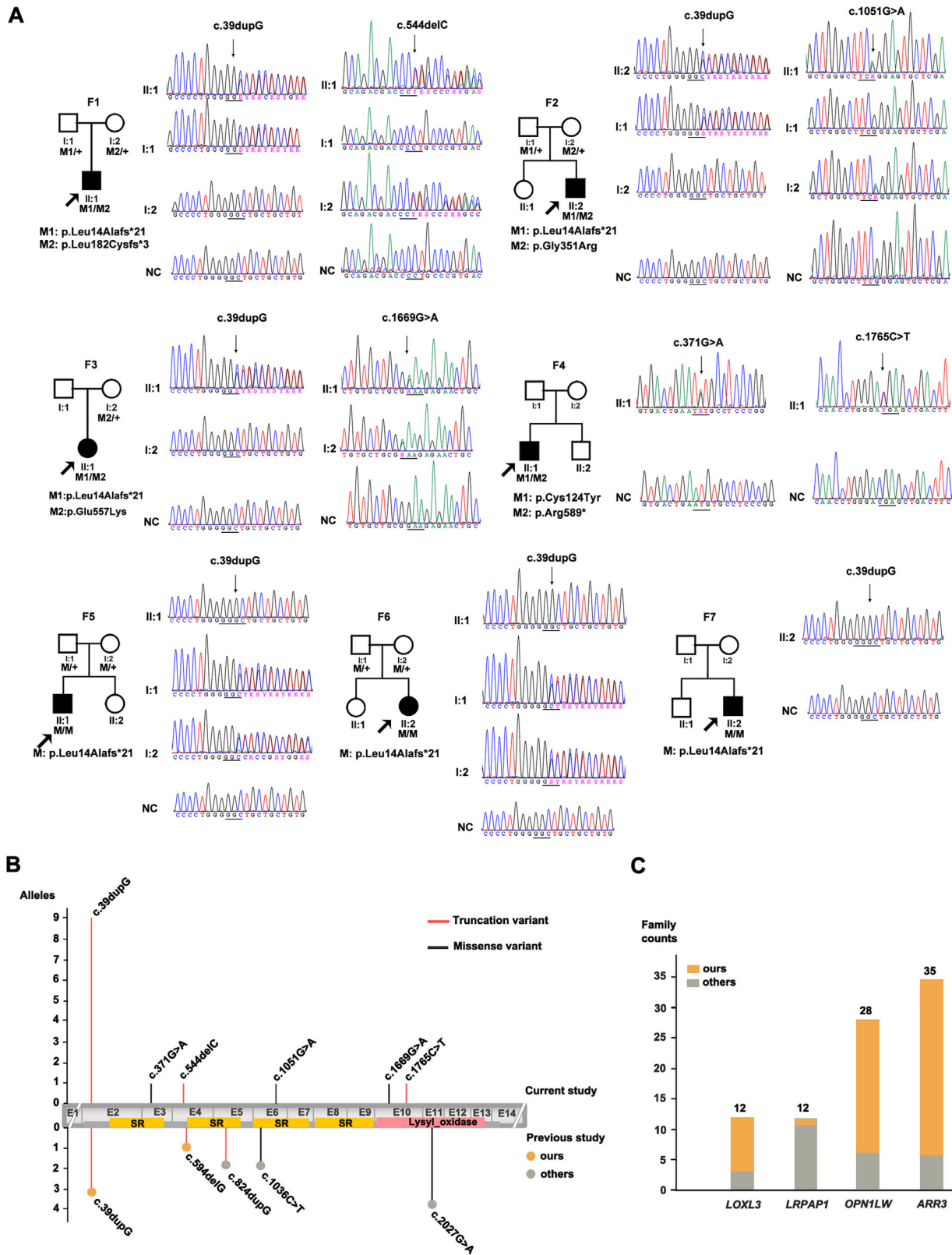


**FIGURE 1.** The distribution of biallelic *LOXL3* variants and genetic landscape of Mendelian coHM based on in-house cohort and previous studies. **(A)** The pedigrees and sequencing chromatograph of seven new families with biallelic *LOXL3* variants in this study. The biallelic *LOXL3* variants of patients are shown below the pedigrees, and family numbers are shown above the pedigrees. *M* indicates the variant site, and *plus sign* indicates the normal allele. The *filled squares* (male) and *circles* (female) represent the affected individuals. The *black arrow* points at the proband. **(B)** The frequency and distribution of pathogenic or likely pathogenic variants in *LOXL3* in mRNA sequences are based on the current study and HGMD database. (Accession number NM\_032603.5). The *LOXL3* variants identified in this study are located above the sequence and in previous pieces of literature are located below the sequence. The *orange-filled pattern* represents *LOXL3* variants

reported in our previous study; the *gray-filled pattern* represents *LOXL3* variants reported in other previous studies. The *red line* indicates the truncation variants, and the *black line* indicates the missense variants. (C) The genetic contribution of four genes (*ARR3*, *OPN1LW*, *LRPAP1*, and *LOXL3*) to eoHM. The *bar plots* show the counts of families with likely pathogenic variants in these four genes based on in-house data and previous studies. The *orange area* represents families in our cohort, and the *gray area* represents reported families in other previous studies.

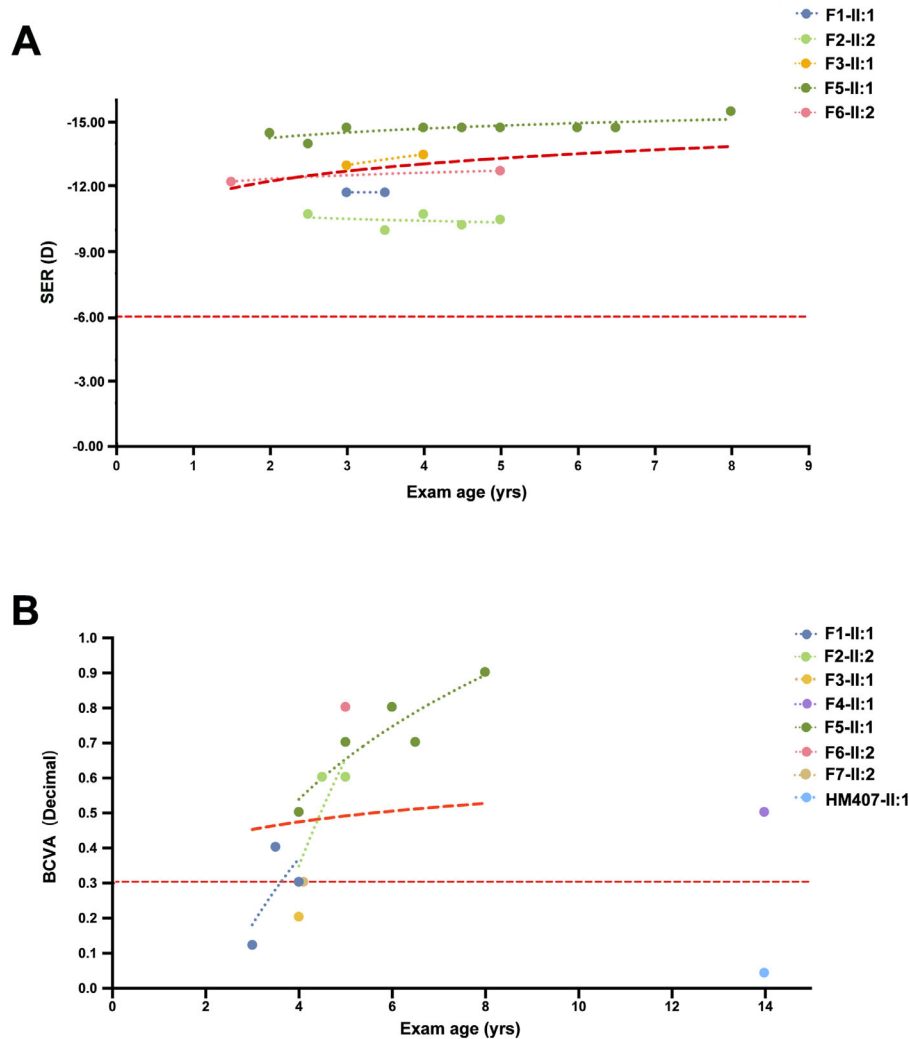


**FIGURE 2.** The distribution and progression of spherical equivalent refractive error in the right eye and of best corrected visual acuity for patients with biallelic *LOXL3* variants in our cohort. (A) The *scatter plot* shows the spherical-equivalent refractive error (SER) distribution and progression of five patients with biallelic *LOXL3* variants. The *light red dotted line* represents SER of  $-6.00$  diopters, indicating the lower limit of high myopia refraction. The *red dashed curve* is the best nonlinear fit of all data points, which demonstrates the slow SER progression with age. (B) The *scatter plot* shows the BCVA changing with the age of eight patients with biallelic *LOXL3* variants. The *light red dotted line* represents BCVA of 0.3 decimal, indicating the legal upper limit of low vision. The *red dashed line* represents the best nonlinear fit of all data points, which demonstrates the slow improvement in BCVA with age.

Table 2). The fundus autofluorescence pictures show an inconspicuous hypofluorescence spot in the foveal area. No characteristic vitreous abnormalities such as membranous or beaded vitreous anomalies were observed in these patients. The available OCT scans revealed Grade I to Grade II foveal hypoplasia in three patients (Fig. 3). The available ERG examination results demonstrated a mild reduction in cone response (Figs. 4B–D). For the extraocular features, no remarkable skeletal findings were observed, including slipped epiphysis or Legg-Perthes-like disease;

scoliosis, spondylolisthesis, Scheuermann-like kyphotic deformity, or osteoarthritis before age 40. The available radiography images showed nonsignificant changes in the knee and elbow joints of two probands (F5-II:1 and F7-II:2) (Fig. 5; Supplementary Fig. S3). The available audiological evaluation was normal (from 0 to 20 dB HL across the frequency range) (Supplementary Figs. S3I–L). Additionally, these patients did not exhibit noticeable orofacial abnormalities, including flat midface, cleft palate, or micrognathia (Supplementary Figs. S3A–H).



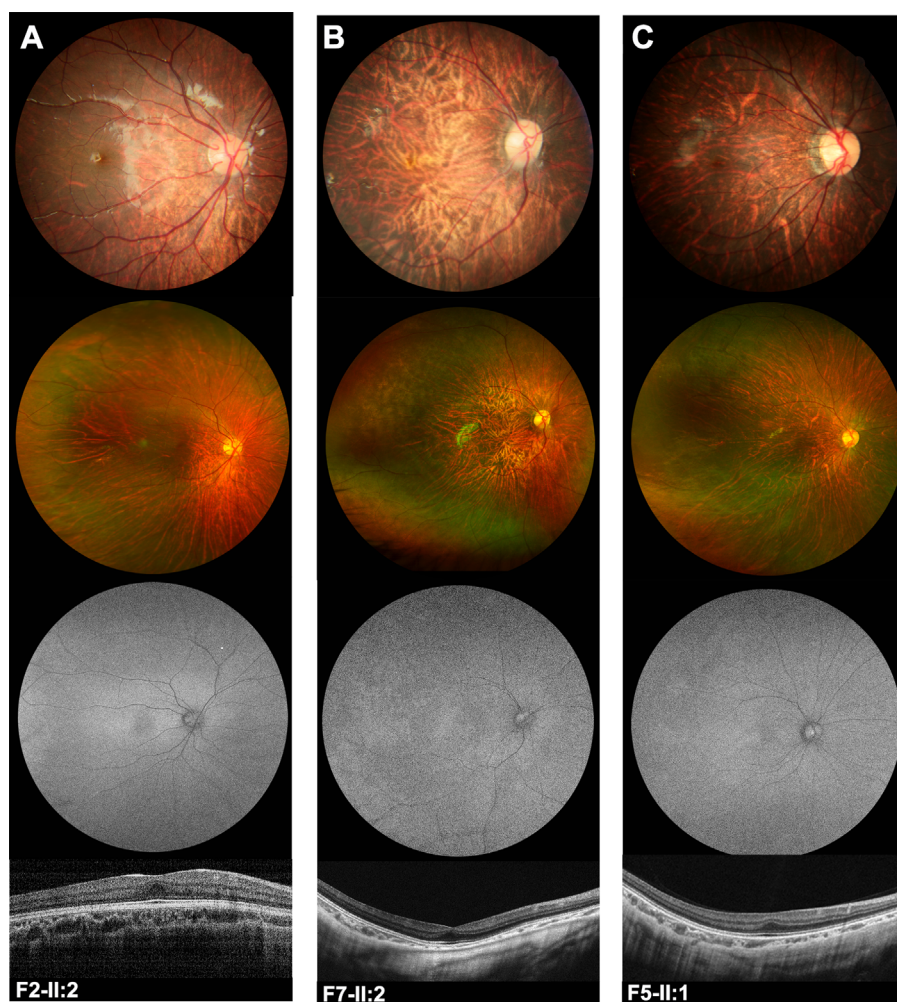


**FIGURE 3.** The fundus images and optical coherence tomography scans of three patients in this study. (A, B) The traditional fundus images of patients (F2-II:2 and F7-II:2) showed the tessellated fundus. The OCT scans demonstrate Grade I foveal hypoplasia. (C) The traditional fundus images of the patient (F5-II:1) show the tessellated fundus and peripapillary crescent in the right eye. The OCT scans demonstrate Grade II foveal hypoplasia. The ultra-widefield fundus images of these three patients also reveal typical myopic fundus changes and no signs of radial perivascular chorioretinal degeneration, circumferential lattice degeneration, or radial lattice degeneration are observed in the right eyes. No other changes are observed except for the faint hypofluorescent spots in the fovea area in the fundus autofluorescence photographs of these three patients, which is consistent with clinical findings in high myopia but not similar to cone-rod dystrophy or retinitis pigmentosa.

## DISCUSSION

In the current study, seven pathogenic or likely pathogenic *LOXL3* variants were screened from in-house exome sequencing data of 8389 patients with different eye conditions. The biallelic *LOXL3* pathogenic variants occurred exclusively in nine unrelated patients with the same phenotype (eoHM), which provided solid evidence of association of MYP28 with *LOXL3* ( $P = 2.97 \times 10^{-8}$ , Fisher's exact test;  $P = 3.81 \times 10^{-6}$ , transmission disequilibrium test). The exclusion of variants in other known genes responsible for nonsyndromic and syndromic Mendelian high myopia provides additional support. All nine patients from the nine families had at least one allele with truncation variants, including six with biallelic truncations and three with one truncation allele and one missense, which are different from the two cases with biallelic missense variants and Stickler syndrome. For all nine cases in nine unrelated families from our cohort, the manifestation of eoHM is the only main and consistent feature that firmly confirms the causative

roles of biallelic *LOXL3* variants in the development of MYP28.

*LOXL3*-associated MYP28 is likely a common form of autosomal recessive eoHM. To date, three loci (MYP18, OMIM 255500; MYP23, OMIM 615431; MYP28, OMIM 619781) have been reported for autosomal recessive eoHM, of which variants in *LRPAP1* and *LOXL3* have been reported to be responsible for MYP23<sup>8</sup> and MYP28<sup>11</sup>, respectively. So far, variants in *LRPAP1* and *LOXL3* have been reported in 12 families each (Fig. 1C).<sup>8,10-13,26,28-30</sup> These data together with our recently reported data<sup>32</sup> suggest that MYP28 ranks the third position for eoHM with identified variants, following the MYP26 because of the *ARR3* variant and MYP1 because of the *OPN1LW* variant. Hence, the findings of the present study support that the *LOXL3*-associated MYP28 represents the common type of autosomal recessive extreme eoHM and provide clues into *LOXL3*-associated with MYP28 in two main ways, including molecular basis, as well as clinical characteristics, which will have important implications for the treatment and diagnosis of eoHM.

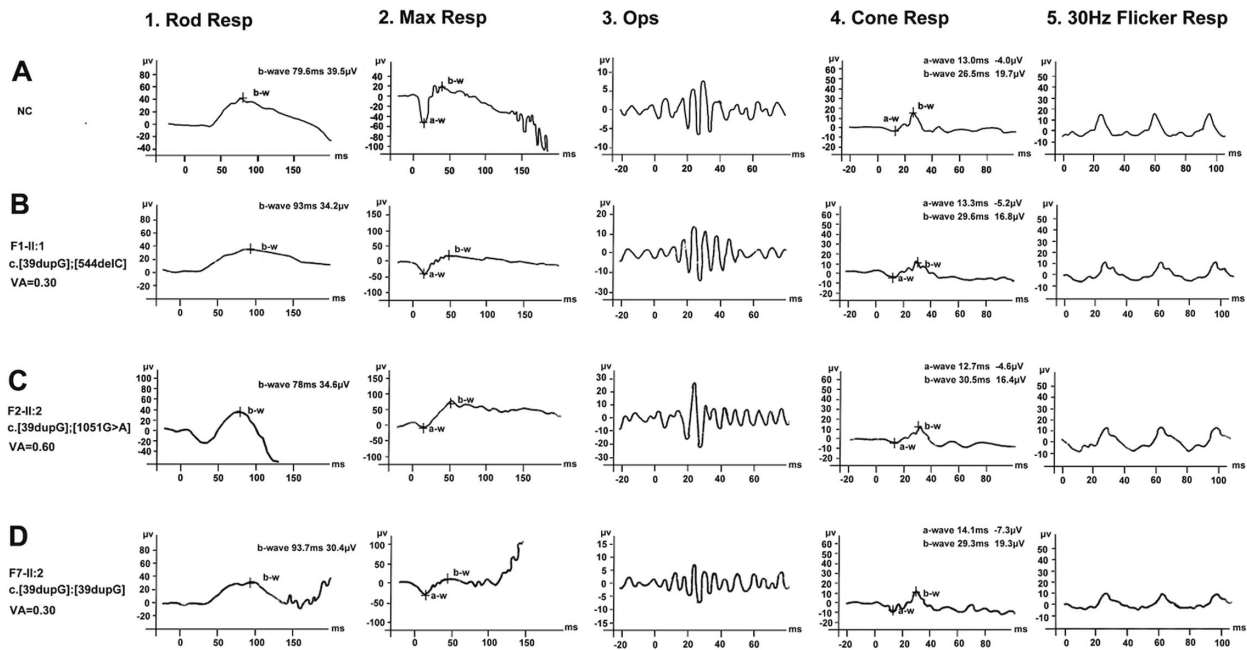


FIGURE 4. The ERG recordings of right eyes in three patients with biallelic *LOXL3* variants. (A) The ERG results from a normal control eye. (B–D) The ERG findings of three patients (F1-II:1, F2-II:2, and F7-II:2) reveal the mild reduction of cone responses and normal rod responses.

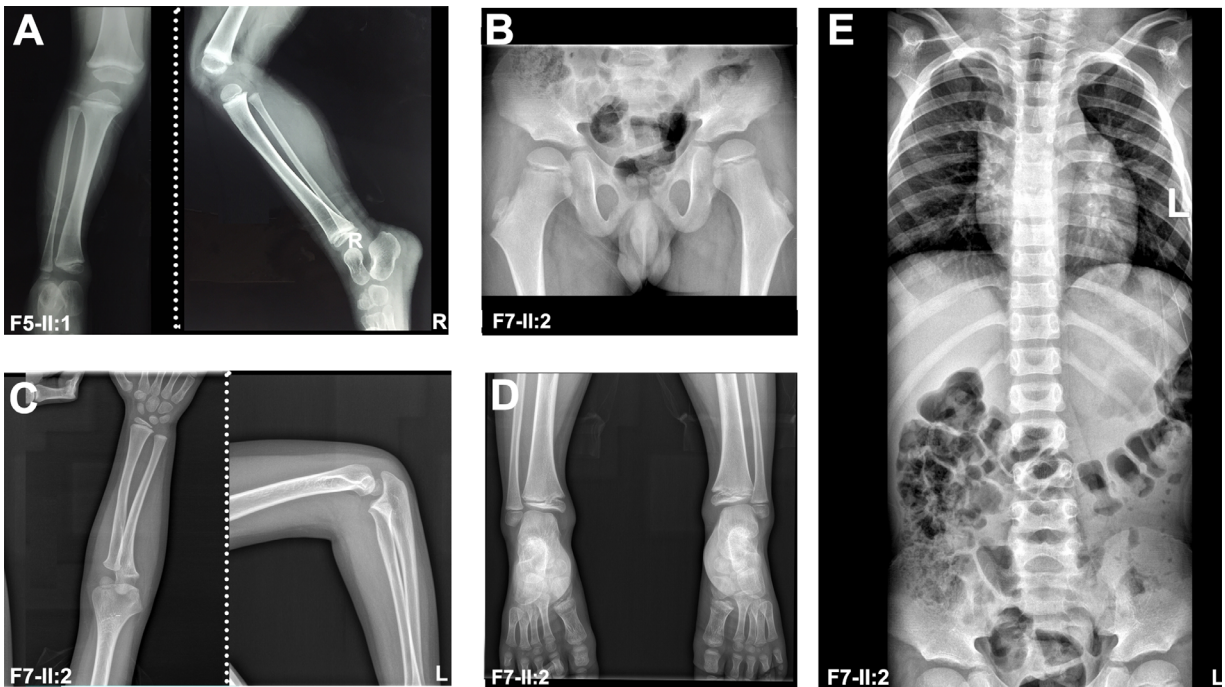


FIGURE 5. The X-ray images of two patients with likely pathogenic variants in *LOXL3*. (A) The X-ray films of the knee and ankle of the proband (F5-II:1) show genu valgum. (B–D) Pelvis, elbow, wrist, and ankle joint radiographs of the proband F7-II:2 reveal nonspecific changes. (E) The X-ray film of the spine of the proband F7-II:1 shows no abnormalities.

In contrast to the clinical data observed in more than 100 cases of Stickler syndrome with variants in *COL2A1* or *COL11A1* in our clinic, the nine patients with biallelic *LOXL3* variants only had extreme eoHM as a constant

feature but without typical signs observed in Stickler syndrome, including vitreous changes or retinal abnormalities (lattice degeneration, retinal hole, retinal detachment, or retinal tear), cleft palate, characteristic facial features,



high-frequency sensorineural hearing loss, skeletal findings (such as slipped epiphysis or Legg-Perthes-like disease; scoliosis, spondylolisthesis, or Scheuermann-like kyphotic deformity; osteoarthritis before age 40).<sup>33–35</sup> For the extraocular manifestations, no significant skeletal abnormalities, midface development, palate malformation was observed in these nine patients as described in the result. The available auditory evaluation was normal, and the X-ray images demonstrated nonsignificant changes. For the ophthalmologic presentations, except for two patients who had retinal detachment due to ocular trauma, the ultra-wide-field fundus imaging showed typical myopic fundi but without circumferential or radial lattice degeneration.<sup>36–38</sup> The vitreous opacity is also the key to the diagnosis of Stickler syndrome, consisting of two main subgroups: membranous and beaded vitreous anomalies.<sup>39</sup> Nevertheless, such characteristic vitreous abnormalities were absent in our patients at the age of examination. Although it is apparent that eoHM is the main finding in the nine patients described in the current study, the possibility of Stickler syndrome cannot be totally ruled out because variable phenotypes have been described for Stickler syndrome, in which atypical phenotypes may mimic eoHM in some cases as we described before.<sup>40</sup> However, the initial diagnosis of eoHM is preferable for the nine cases at the age of examination in the current study.

Apart from our study (including two previously reported families), so far only five patients in three families have been reported to have biallelic variants in *LOXL3* by other researchers, in which four patients in two families with biallelic missense variants were described to have Stickler syndrome (three of the four patients had eoHM)<sup>10,13</sup> whereas the remaining one with biallelic truncations had eoHM.<sup>12</sup> Except for the difference in phenotypes, however, the genotypes of the nine patients in the current study, biallelic variants with one or two truncations, are different from those reported by the two families with Stickler syndrome. Whether different genotypes contributed to different phenotypes waits to be confirmed in future studies. It has been well recognized in previous studies that missense variants may result in significantly different phenotypes from truncation variants both in dominant and recessive (even one of the two alleles) diseases, as seen in our previous studies on hereditary eye diseases with mutations in *PAX6*,<sup>41</sup> *CPAMD8*,<sup>42</sup> or *RPE65*.<sup>43</sup> Admittedly, some clinical features related to Stickler syndrome may occur or become more obvious in the teenage period, such as vitreous opacity, peripheral retinal lattice degeneration, and part of skeletal findings.<sup>44,45</sup> As seen in the nine patients described in the current study, eoHM appears to be the predominant finding at the age of examination. However, further validation of these findings would require long-term follow-up and observation of the relevant phenotypes.

Except for the aspects mentioned above, *LOXL3*-associated MYP28 has been found to own unique characteristics, which is different from other common types of Mendelian eoHM such as *LRPAP1*-associated MYP23 and *ARR3*-associated MYP26. Initially, the extreme high myopia has been identified as the main clinical manifestation in *LOXL3*-associated MYP28 in the current study. All carriers in this study had an extremely high degree of refraction (at least  $-10.75$  diopters) at the first visit and showed nonprogressive high myopia with age. The degree of myopic refraction in *LOXL3*-associated MYP28 ( $-14.99 \pm 4.06$  diopters) at the first visit is comparatively more severe than in *ARR3*-associated MYP26 ( $-12.58 \pm 4.83$  diopters) as previously

described,<sup>6</sup> but comparatively milder than in *LRPAP1*-associated MYP23 ( $-17$  diopters or greater).<sup>8</sup> In addition, progression of the myopia is slower in MYP28 than in MYP26.<sup>6</sup> The clinical appearance of the retina in MYP28 only demonstrated typical myopic fundus changes, as well as the milder grade of myopic maculopathy, including a tessellated fundus (C1) and diffuse atrophy (C2), based on META-PM classification.<sup>16</sup> Subsequently, as described previously, no noticeable changes were observed in FAF images of patients with *LOXL3* variants in our study, except for the insignificant hypofluorescent spot in the fovea area, which were different from the FAF manifestations of cone-rod dystrophy, retinitis pigmentosa, and Stickler syndrome.<sup>46–48</sup> Besides, the ERG changes in these patients only demonstrated a mild reduction in cone response, which is consistent with ERG changes in high myopia<sup>49,50</sup> and similar to or even milder than the ERG changes in *ARR3*-associated MYP26.<sup>6</sup> The available OCT images demonstrated Grade I to Grade II foveal hypoplasia in three patients. However, according to the regular follow-up examination results, all patients have progressive BCVA with age, and nobody has been observed to have nystagmus. Even these three patients with foveal hypoplasia have fairly good visual acuity based on the latest examination, which is consistent with the hypothesis suggested by Marmor et al.<sup>51</sup> that the foveal pit is not the indispensable condition for the development of foveal cone specialization, either anatomically or functionally. In this study, rhegmatogenous retinal detachment caused by ocular trauma had been observed in two teenagers with *LOXL3*-associated MYP28, indicating that patients with MYP28 might have a high risk of retinal detachment at a young age.

The contribution of genetic factors to high myopia has been postulated for a long time. Through whole-exome sequencing and whole-genome sequencing, rare variants in several genes including *ARR3*, *LOXL3*, *LRPAP1*, *CCDC111*, *NDUFAF7*, *P4HA2*, *SCO2*, *UNC5D*, *BSG*, *SLC39A5*, *CTSH*, and *ZNF644*, have been identified to cause myopia.<sup>3,52</sup> The majority of these genes are autosomal inherited, and several genes were inherited in other inheritance patterns. Based on our recent study and previous studies, *LOXL3* and *LRPAP1* are considered the potential causative genes for autosomal recessive high myopia.<sup>52</sup> Indeed, these two genes both belong to the TGF-beta signaling pathway. *LOXL3*, a copper-dependent amine oxidase, has been reported to contribute to the crosslinking of collagen and elastin in the extracellular matrix (ECM), which can enhance the stiffness and stabilization of ECM.<sup>53</sup> The TGF-beta mediated both SMAD and JNK signaling pathways can induce the expression of *LOXL3*.<sup>54,55</sup> Besides, *LRPAP1* encodes chaperone of lipoprotein receptor-related proteins LRP1 and the deficiency of LRP1 can perturb the TGF-beta regulation.<sup>8</sup> Coincidentally, convincing evidence suggested that TGF- $\beta$  expression plays an essential role in the modulation of ECM in the sclera, leading to the elongation of the ocular axis, enlargement of eye size, and the development of myopia.<sup>56</sup>

In conclusion, the current study found that biallelic *LOXL3* variants were exclusively enriched in nine patients with eoHM, providing firm evidence to support that causative association between biallelic *LOXL3* variants and MYP28. The current study showed that *LOXL3*-associated MYP28 ranked third among Mendelian eoHM with identified variants, suggesting that MYP28 is a common form of autosomal recessive eoHM. Furthermore, extreme eoHM is the only constant and main feature of *LOXL3*-associated MYP28. The results of this study further deepen our understanding

of the clinical and genetic landscape of *LOXL3*-associated MYP28. Moreover, identification of the genes that contribute to Mendelian eoHM, particularly in common forms, is an invaluable initial step toward understanding the molecular mechanism underlying high myopia, as well as common myopia.

### Acknowledgments

The authors are grateful to all patients and members of their families for their participation in this study.

Supported by grants from the National Natural Science Foundation of China (81770965), the Science and Technology Planning Projects of Guangzhou (202102010271), and the Fundamental Research Funds of the State Key Laboratory of Ophthalmology.

Disclosure: **Y. Jiang**, None; **L. Zhou**, None; **Y. Wang**, None; **J. Ouyang**, None; **S. Li**, None; **X. Xiao**, None; **X. Jia**, None; **J. Wang**, None; **Z. Yi**, None; **W. Sun**, None; **X. Jiao**, None; **P. Wang**, None; **J.F. Hejtmančík**, None; **Q. Zhang**, None

### References

- Flitcroft DI, He M, Jonas JB, et al. IMI - defining and classifying myopia: A proposed set of standards for clinical and epidemiologic studies. *Invest Ophthalmol Vis Sci*. 2019;60:M20–M30.
- Stambolian D. Genetic susceptibility and mechanisms for refractive error. *Clin Genet*. 2013;84:102–108.
- Baird PN, Saw SM, Lanca C, et al. Myopia. *Nat Rev Dis Primers*. 2020;6:99.
- Zhang Q. Genetics of Pathologic Myopia. In: Spaide RF, Ohno-Matsui K, Yannuzzi LA, eds. *Pathologic Myopia*. Cham: Springer International Publishing; 2021:43–58.
- Li J, Zhang Q. Insight into the molecular genetics of myopia. *Mol Vis*. 2017;23:1048–1080.
- Wang Y, Xiao X, Li X, et al. Genetic and clinical landscape of *ARR3*-associated MYP26: The most common cause of Mendelian early-onset high myopia with a unique inheritance [published online ahead of print September 30, 2022]. *Br J Ophthalmol*, doi:10.1136/bjo-2022-321511.
- Zhou L, Xiao X, Li S, Jia X, Zhang Q. Frequent mutations of *RetNet* genes in eoHM: Further confirmation in 325 probands and comparison with late-onset high myopia based on exome sequencing. *Exp Eye Res*. 2018;171:76–91.
- Aldahmesh MA, Khan AO, Alkuraya H, et al. Mutations in *LRPAP1* are associated with severe myopia in humans. *Am J Hum Genet*. 2013;93:313–320.
- Lee JE, Kim Y. A tissue-specific variant of the human lysyl oxidase-like protein 3 (*LOXL3*) functions as an amine oxidase with substrate specificity. *J Biol Chem*. 2006;281:37282–37290.
- Alzahrani F, Al Hazzaa SA, Tayeb H, Alkuraya FS. *LOXL3*, encoding lysyl oxidase-like 3, is mutated in a family with autosomal recessive Stickler syndrome. *Hum Genet*. 2015;134:451–453.
- Li J, Gao B, Xiao X, et al. Exome sequencing identified null mutations in *LOXL3* associated with early-onset high myopia. *Mol Vis*. 2016;22:161–167.
- Maddirevula S, Shamseldin HE, Sirr A, et al. Exploiting the autozygome to support previously published mendelian gene-disease associations: An update. *Front Genet*. 2020;11:580484.
- Chan TK, Alkaabi MK, ElBarky AM, El-Hattab AW. *LOXL3* novel mutation causing a rare form of autosomal recessive Stickler syndrome. *Clin Genet*. 2019;95:325–328.
- Wang Q, Wang P, Li S, et al. Mitochondrial DNA haplogroup distribution in Chaoshanese with and without myopia. *Mol Vis*. 2010;16:303–309.
- Thomas MG, Kumar A, Mohammad S, et al. Structural grading of foveal hypoplasia using spectral-domain optical coherence tomography a predictor of visual acuity? *Ophthalmology*. 2011;118:1653–1660.
- Ohno-Matsui K, Kawasaki R, Jonas JB, et al. International photographic classification and grading system for myopic maculopathy. *Am J Ophthalmol*. 2015;159:877–883.e877.
- Li J, Jiang D, Xiao X, et al. Evaluation of 12 myopia-associated genes in Chinese patients with high myopia. *Invest Ophthalmol Vis Sci*. 2015;56:722–729.
- Wang P, Li S, Sun W, et al. An ophthalmic targeted exome sequencing panel as a powerful tool to identify causative mutations in patients suspected of hereditary eye diseases. *Transl Vis Sci Technol*. 2019;8:21.
- Xiao S, Sun W, Xiao X, et al. Clinical and genetic features of retinoschisis in 120 families with *RS1* mutations. *Br J Ophthalmol*. 2023;107:367–372.
- Chen Y, Zhang Q, Shen T, et al. Comprehensive mutation analysis by whole-exome sequencing in 41 Chinese families with Leber congenital amaurosis. *Invest Ophthalmol Vis Sci*. 2013;54:4351–4357.
- Zhang Q, Zulfiqar F, Xiao X, et al. Severe autosomal recessive retinitis pigmentosa maps to chromosome 1p13.3-p21.2 between *D1S2896* and *D1S457* but outside *ABCA4*. *Hum Genet*. 2005;118:356–365.
- Liu F, Wang J, Xing Y, Li T. Mutation screening of 17 candidate genes in a cohort of 67 probands with early-onset high myopia. *Ophthalmic Physiol Opt*. 2020;40:271–280.
- Széll N, Fehér T, Maróti Z, et al. Myopia-26, the female-limited form of early-onset high myopia, occurring in a European family. *Orphanet J Rare Dis*. 2021;16:45.
- Xiao X, Li S, Jia X, Guo X, Zhang Q. X-linked heterozygous mutations in *ARR3* cause female-limited early onset high myopia. *Mol Vis*. 2016;22:1257–1266.
- van Mazijk R, Haarman AEG, Hoefsloot LH, et al. Early onset X-linked female limited high myopia in three multigenerational families caused by novel mutations in the *ARR3* gene. *Hum Mutat*. 2022;43:380–388.
- Ceyhan-Birsoy O, Murry JB, Machini K, et al. Interpretation of genomic sequencing results in healthy and ill newborns: Results from the BabySeq Project. *Am J Hum Genet*. 2019;104:76–93.
- Yuan D, Yan T, Luo S, et al. Identification and functional characterization of a novel nonsense variant in *ARR3* in a Southern Chinese family with high myopia. *Front Genet*. 2021;12:765503.
- Jiang D, Li J, Xiao X, et al. Detection of mutations in *LRPAP1*, *CTSH*, *LEPREL1*, *ZNF644*, *SLC39A5*, and *SCO2* in 298 families with early-onset high myopia by exome sequencing. *Invest Ophthalmol Vis Sci*. 2014;56:339–345.
- Khan AO, Aldahmesh MA, Alkuraya FS. Clinical characterization of *LRPAP1*-related pediatric high myopia. *Ophthalmology*. 2016;123:434–435.
- Magliyah MS, Alsulaiman SM, Nowilaty SR, Alkuraya FS, Schatz P. Rhegmatogenous retinal detachment in nonsyndromic high myopia associated with recessive mutations in *LRPAP1*. *Ophthalmol Retina*. 2020;4:77–83.
- Mountford JK, Davies WIL, Griffiths LR, Yazar S, Mackey DA, Hunt DM. Differential stability of variant *OPN1LW* gene transcripts in myopic patients. *Mol Vis*. 2019;25:183–193.
- Wang J, Wang Y, Li S, et al. Clinical and genetic analysis of *RDH12*-associated retinopathy in 27 Chinese families: A hypomorphic allele leads to cone-rod dystrophy. *Invest Ophthalmol Vis Sci*. 2022;63:24.
- Robin NH, Moran RT, Ala-Kokko L. *Stickler syndrome*. 1993.

34. Nixon TRW, Richards AJ, Martin H, Alexander P, Snead MP. Autosomal recessive Stickler syndrome. *Genes*. 2022;13:1135.
35. Snead MP, Yates JR. Clinical and molecular genetics of Stickler syndrome. *J Med Genet*. 1999;36:353–359.
36. Edwards AO. Clinical features of the congenital vitreo-retinopathies. *Eye (Lond)*. 2008;22:1233–1242.
37. Vu CD, Brown J, Jr., Körkkö J, Ritter R, 3rd, Edwards AO. Posterior chorioretinal atrophy and vitreous phenotype in a family with Stickler syndrome from a mutation in the COL2A1 gene. *Ophthalmology*. 2003;110:70–77.
38. Van Camp G, Snoeckx RL, Hilgert N, et al. A new autosomal recessive form of Stickler syndrome is caused by a mutation in the COL9A1 gene. *Am J Hum Genet*. 2006;79:449–457.
39. Soh Z, Richards AJ, McNinch A, Alexander P, Martin H, Snead MP. Dominant Stickler syndrome. *Genes*. 2022;13:1089.
40. Zhou L, Xiao X, Li S, et al. Phenotypic characterization of patients with early-onset high myopia due to mutations in COL2A1 or COL11A1: Why not Stickler syndrome? *Mol Vis*. 2018;24:560–573.
41. Jiang Y, Li S, Xiao X, Sun W, Zhang Q. Genotype-phenotype of isolated foveal hypoplasia in a large cohort: Minor iris changes as an indicator of PAX6 involvement. *Invest Ophthalmol Vis Sci*. 2021;62:23.
42. Li X, Sun W, Xiao X, et al. Biallelic variants in CPAMD8 are associated with primary open-angle glaucoma and primary angle-closure glaucoma. *Br J Ophthalmol*. 2022;106:1710–1715.
43. Li S, Xiao X, Yi Z, Sun W, Wang P, Zhang Q. RPE65 mutation frequency and phenotypic variation according to exome sequencing in a tertiary centre for genetic eye diseases in China. *Acta Ophthalmol*. 2020;98:e181–e190.
44. Hanson-Kahn A, Li B, Cohn DH, Nickerson DA, Bamshad MJ, Hudgins L. Autosomal recessive Stickler syndrome resulting from a COL9A3 mutation. *Am J Med Genet A*. 2018;176:2887–2891.
45. Liberfarb RM, Levy HP, Rose PS, et al. The Stickler syndrome: Genotype/phenotype correlation in 10 families with Stickler syndrome resulting from seven mutations in the type II collagen gene locus COL2A1. *Genet Med*. 2003;5:21–27.
46. Oishi A, Oishi M, Ogino K, Morooka S, Yoshimura N. Wide-field fundus autofluorescence for retinitis pigmentosa and cone/cone-rod dystrophy. *Adv Exp Med Biol*. 2016;854:307–313.
47. Pichi F, Abboud EB, Ghazi NG, Khan AO. Fundus autofluorescence imaging in hereditary retinal diseases. *Acta Ophthalmol*. 2018;96:e549–e561.
48. Fujimoto K, Nagata T, Matsushita I, et al. Ultra-wide field fundus autofluorescence imaging of eyes with stickler syndrome. *Retina*. 2021;41:638–645.
49. Wang P, Xiao X, Huang L, Guo X, Zhang Q. Cone-rod dysfunction is a sign of early-onset high myopia. *Optom Vis Sci*. 2013;90:1327–1330.
50. Gupta SK, Chakraborty R, Verkicharla PK. Electroretinogram responses in myopia: A review. *Adv Ophthalmol*. 2022;145:77–95.
51. Marmor MF, Choi SS, Zawadzki RJ, Werner JS. Visual insignificance of the foveal pit: Reassessment of foveal hypoplasia as fovea plana. *Arch Ophthalmol*. 2008;126:907–913.
52. Tedja MS, Haarman AEG, Meester-Smoor MA, et al. IMI - myopia genetics report. *Invest Ophthalmol Vis Sci*. 2019;60:M89–M105.
53. Laurentino TS, Soares RDS, Marie SKN, Oba-Shinjo SM. LOXL3 function beyond amino oxidase and role in pathologies, including cancer. *Int J Mol Sci*. 2019;20.
54. Sethi A, Wordinger RJ, Clark AF. Gremlin utilizes canonical and non-canonical TGFβ signaling to induce lysyl oxidase (LOX) genes in human trabecular meshwork cells. *Exp Eye Res*. 2013;113:117–127.
55. Sethi A, Mao W, Wordinger RJ, Clark AF. Transforming growth factor-beta induces extracellular matrix protein cross-linking lysyl oxidase (LOX) genes in human trabecular meshwork cells. *Invest Ophthalmol Vis Sci*. 2011;52:5240–5250.
56. Jobling AI, Nguyen M, Gentle A, McBrien NA. Isoform-specific changes in scleral transforming growth factor-beta expression and the regulation of collagen synthesis during myopia progression. *J Biol Chem*. 2004;279:18121–18126.